

Influence of casting and heat treatment parameters in controlling the properties of an Al-10 wt % Si-0.6 wt % Mg/SiC/20p composite

A. M. SAMUEL, F. H. SAMUEL

Département des Sciences Appliquées, Université du Québec à Chicoutimi, Chicoutimi, Québec, G7H 2B1, Canada

The influence of melting, casting and heat treatment parameters in determining the quality and tensile properties of an Al-10 wt % Si-0.6 wt % Mg/SiC/20p composite in comparison to its base alloy (359) has been studied. For the composite, melt-temperature, hydrogen level, and the cleanliness and stirring procedure, control, respectively, the harmful melt reactions of the SiC reinforcement with the alloy matrix, gas porosity, inclusion and oxide-film contamination, whereas casting conditions are mainly controlled through the use of a proper mold temperature and appropriate mold coating materials that enhance the feedability and reduce or eliminate the effects of shrinkage. The beneficial effect of the SiC reinforcement particles is two-fold: 1. they act as preferential sites for the nucleation of the eutectic silicon particles, leading to an overall refinement of the latter and lowering the amount of strontium modifier required from 150 to 90 ppm to achieve the same level of refinement in the as-cast microstructures of both composite and base alloy; 2. their presence also results in a more uniform redistribution of the silicon particles in the as-cast structure (cf. the large, irregular interdendritic regions of eutectic silicon observed in the base alloy). Both composite and base alloy exhibit a similar heat treatment response with respect to tensile properties for the various heat treatments applied. Addition of 20 vol % SiC to the base alloy (359) is seen to increase the Young's modulus and yield strength by 30–40%, marginally affect the ultimate tensile strength, but reduce the ductility by almost 80%.

1. Introduction

The mechanical properties of a casting are determined chiefly by its chemical composition, the molten metal processing parameters, the casting method involved and the heat treatment applied to it. In the case of particle reinforced composites, the reinforcement particles influence the solidification process in various ways that ultimately affect the fluidity and, hence, castability of the composite. In contrast to the extensive data available on the heat treatment of Al–Si–Mg base (matrix) alloys [1, 2], relatively little is documented for their metal matrix composites [3, 4].

The present work forms part of an extensive programme on SiC particulate reinforced Al–Si–Mg composites being carried out at the Université du Québec à Chicoutimi on various aspects involved in the production of optimum quality castings with corresponding properties. The main purpose of this article is to emphasize the important role of melting and casting procedure on the one hand, and heat treatment variables on the other, in determining the quality and tensile properties of the final product. The results reported here highlight the influence of these parameters.

2. Experimental procedure

The chemical compositions of the two alloys used in the present study are shown in Table I. The composite material was received in the form of 12.5 kg ingots from Duralcan Canada, Usine Dubuc, Chicoutimi, Québec. The ingots were cut into two halves and heated at 400 °C for 2 h prior to remelting. The cut pieces were charged to a 36 kg silicon carbide crucible when the temperature inside the crucible reached 550 °C. To prevent SiC particle sedimentation during remelting, the melt was mechanically stirred using a graphite impeller designed especially for this purpose.

In order to obtain the 359 base (matrix) alloy, the silicon and magnesium levels of 356 alloy were adjusted by adding pure silicon and Al-50 wt % Mg master alloy to an 356 alloy melt. The melt was degassed using a hollow graphite rotary impeller, running at 180 r.p.m., through which dry argon was passed into the melt.

The melt hydrogen level was monitored using an Alscan unit. In addition, for both composite and base alloy melts, specimens were also cast simultaneously in Ransley molds (for each pouring/casting) from which "Ransley" samples were machined for determination

TABLE I Chemical compositions (wt %) of the two alloys studied (based on ICP analysis of at least 35 castings)

Alloy type	Si (wt %)	Mg (wt %)	Fe (wt %)	Cu (wt %)	Mn (wt %)	Ti (wt %)	Sr (wt %)	SiC (vol %)
359	10.2	0.70	0.10	0.018	0.004	0.09	150	–
Composite	9.4	0.59	0.14	0.01	0.004	0.10	90	20.9

of hydrogen content using the Leco vacuum fusion technique. This is one of the standard methods for obtaining accurate analysis of the hydrogen content in a melt [5]. The analysis was carried out at Alcan International's Arvida R&D Centre, Jonquière, P.Q. In both cases, the melt was filtered using ceramic foam filters (of 15 ppi size for the composite and 20 ppi size for the base alloy). Filters [1.5 in (3.3 cm) diameter discs] were placed at the bottom of stainless steel tubes [ca. 7 in (15 cm) in length] that constituted the external risers and which were heated at 600 °C prior to casting. The melt temperature was kept close to 735 °C whereas the mold temperature (Stahl Mold, ASTM-B-108-85a [6]) was about 400–410 °C.

For each pouring, specimens for chemical analysis were taken from the central portion of the crucible. As-cast test bars were subjected to various heat treatments:

1. solution treatment 8 h at 540 °C and 24 h at 550 °C;
2. quenching water at 25 or 60 °C
3. stabilizing at room temperature 0, 24 and 48 h
4. artificial ageing 5 h at 155 °C.

Tensile tests were performed (under uniaxial tensile loading) on specimens taken from these tempered test bars, employing an Instron testing machine and using a strain rate of $4 \times 10^{-4} \text{ s}^{-1}$. All tests were conducted at room temperature, and for each tempered condition a minimum of at least 10 test bar specimens were tested. To examine the casting defects, longitudinal samples were sectioned from the fractured test bars. All samples were polished using a technique specially developed for such composites.

Metallographic samples (transverse sections) were also obtained from the central (gauge length) portions of the tensile tested test bars from positions away from the fracture surface to examine the microstructural characteristics, using optical (Olympus PMG3) and scanning electron microscopy. Porosity and oxide volume fractions, as well as eutectic silicon particle characteristics, were measured using image analysis (Leco 2001 image analyser system attached to the optical microscope), carried out in the usual manner as that employed for volume fraction or other measurements of any specified phase (see Refs [7] and [8] for details).

3. Results and discussion

3.1. Casting conditions

3.1.1. Feeding

Fig. 1 shows the gauge length features of three different test bars marked A, B and C. Bars B and C,

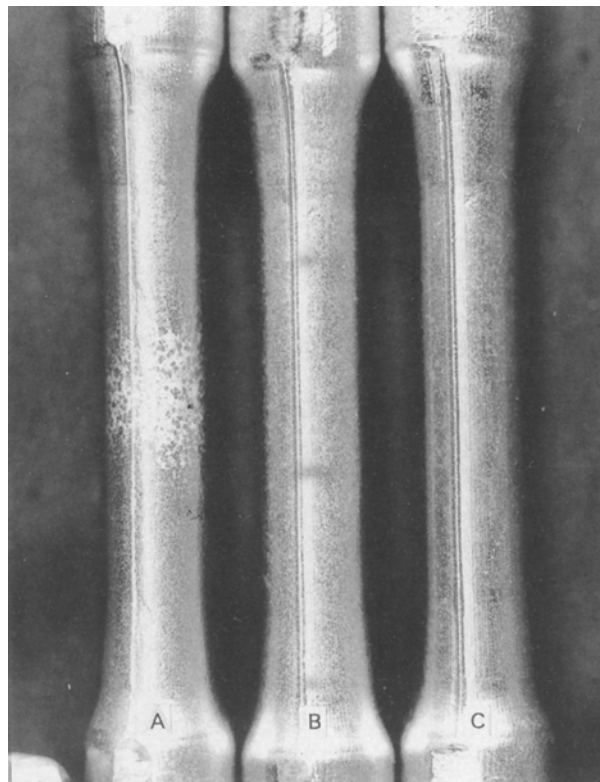


Figure 1 Gauge length of test bars obtained from Stahl mold castings: A = unfiltered composite; B = filtered composite; C = filtered 359 alloy.

composite and base alloy samples, respectively, were produced using the experimental procedures described above. Bar A, produced from the same composite, was obtained without the use of filtration. A large, shrinkage-defect area extending over almost 2 cm can be seen at the centre of the latter, whereas, by comparison, bars B and C display a much better defect-free surface quality. Application of the present technique, i.e. the use of an external preheated riser (stainless steel tube), results in a significant improvement in the shrinkage due to proper feeding through the pressure supplied by the molten metal in the riser. This simple process was found to be adequate enough to produce composite test bars (bar B) of a quality equal to those obtained from the base alloy (bar C).

The coating applied to the inner walls of a mold is an important parameter in controlling the quality of the end product. Test bars B and C (Fig. 1) were obtained from molds where the mold walls were coated with a thick layer (100–150 μm) of vermiculite (refractory insulating material dissolved in a water sodium silicate base), as shown schematically in Fig. 2. This type of coating reduces the heat transfer rate,

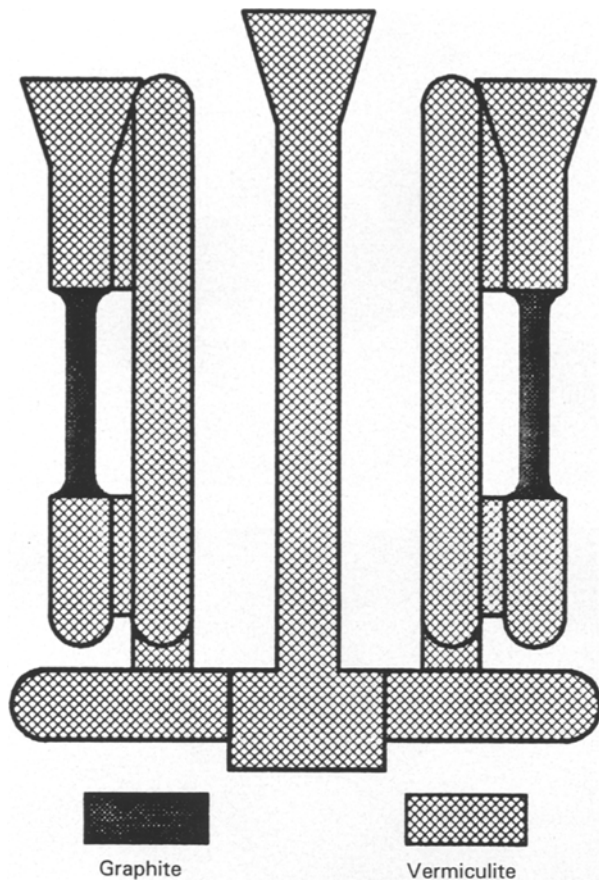


Figure 2 Schematic diagram of the Stahl mold used in the present work showing the distribution of coating.

which in turn allows hot metal with proper fluidity to enter into the casting (test bar) cavities. The gauge length part of the mold, however, was coated with a thin layer of graphite (ca. $50\ \mu\text{m}$) to enhance the cooling rate and, hence, decrease the gas porosity obtained.

Fig. 3a, an optical micrograph taken from the area beneath the fracture surface of test bar A of Fig. 1, shows a large amount of gas and shrinkage porosity. The porosity volume fraction, as measured by image analysis, was found to be ca. 2.5%. In such cases, when the porosity volume fractions were of this order, the corresponding test bars failed before reaching the yield point, i.e. they displayed zero (or no) ductility.

The corresponding microstructure for test bar B of Fig. 1, Fig. 3b, revealed a much reduced porosity volume fraction, ca. 0.4% (as obtained from image analysis). The round shape of the pores observed in this figure indicate that these pores are mainly gas type (the hydrogen level being ca. $0.14\ \text{ml}/100\ \text{g Al}$ in this case). Even with this amount of porosity, the attainable tensile properties in the T6-condition (8 h solutionizing at 540°C /water quench at $60^\circ\text{C}/5\ \text{h}$ ageing at 155°C) are YS ca. 49 ksi, UTS ca. 53 ksi and El% ca. 0.6%.

Fig. 3c shows the corresponding microstructure obtained from the area beneath the fracture surface of test bar C. As can be seen, the dendrite arm spacing is uniform throughout the microstructure, with almost no sign of either gas or shrinkage porosity (the total porosity volume fraction was determined to be ca.

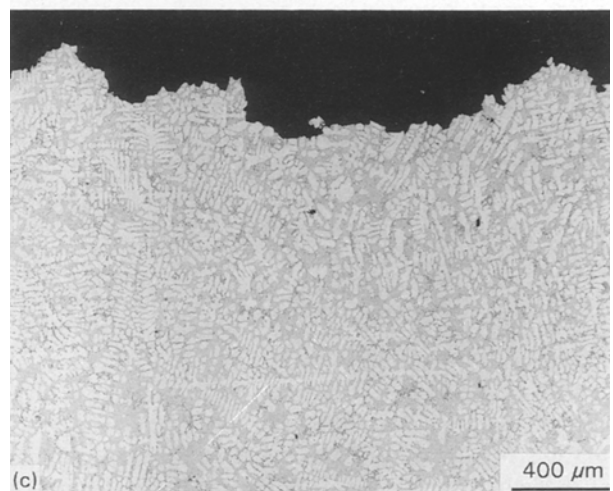
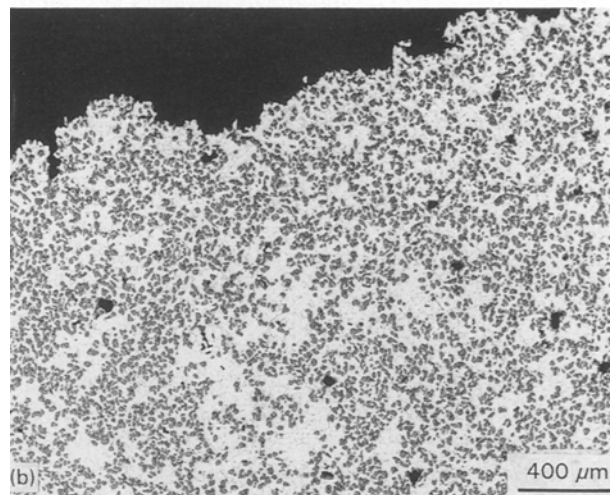
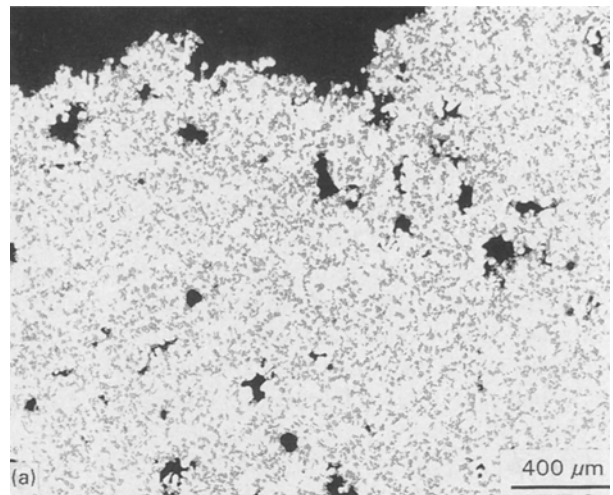


Figure 3 Microstructure beneath the fracture surface of samples (a), (b) and (c), corresponding to test bars A, B and C of Fig. 1.

0.01%). The obtained mechanical properties were YS ca. 41 ksi, UTS ca. 48 ksi, El ca. 4%.

From the results obtained for the base alloy (test bar C), it may reasonably be presumed that degassing the composite melts would result in a marked improvement in their tensile properties through a reduction in the gas porosity. However, degassing of such composites using the conventional methods reportedly results in the loss and dewetting of the reinforcement particles. Recently, Provencher *et al.* [9]

have included fluxing/degassing in the recycling and remelting procedures proposed by them for Duralcan foundry composites (of the type used in the present study), they report that the injection of a (argon + 15% SF₆) gas mixture in the melt, in the vicinity of an impeller that provides a sufficient shearing action to give proper bubble size and distribution within the melt, oxide films and hydrogen may be removed from the melt, while the reinforcement particles remain dispersed within the melt. A critical combination of impeller shear action and gas flow rate is required, without which improper fluxing/degassing will occur, in which case lowered fluidity and mechanical properties are observed.

Rose *et al.* [10] have also reported on the degassing and cleaning of these composites. According to them, the use of an active gas results in partial or substantial loss of the reinforcement particles. This effect was observed even at low concentrations of the active gas (e.g. less than 3% chlorine or 6% SF₆) in argon, which led them to use only pure and dry argon as the degassing/cleaning medium. Based on their trials, the authors have proposed a procedure following the necessary steps of which mechanical properties consistent with those reported for fresh-ingot material are observed.

Yet another problem associated with improper feeding in the case of the composite appears to be the presence of clusters of the SiC particulates, an example of which is shown in Fig. 4a, where clusters of SiC particles are seen separated from each other by large voids. A high magnification scanning electron micrograph of this specimen, Fig. 4b, reveals that these voids result from the lack of metal flow in the gaps between adjacent reinforcement particles. The small particles clearly visible on some of the SiC particles are believed to be spinel (MgAl₂O₄ phase). The 0.65 wt % Mg content of the present composite would favour/enhance the formation of this phase more than that of MgO [11]. Formation of spinel reaction is further elaborated upon in Section 3.1.3.

3.1.2. Porosity and oxide content

Porosity and oxides have a detrimental effect on the tensile properties of a casting. Thus, a correct measurement of their volume fractions is crucial in estimating any quantitative correlation between the two.

In their quantitative evaluation of the melt quality (as assessed by the presence of oxide films and the hydrogen/porosity level), Provencher *et al.* [9] utilized "Ransley" samples (depicted a) in Fig. 5) for metallographic observations of both porosity and oxide content of their composite samples. According to them, such Ransley samples displayed, "good metallographic quality and reproducibility of results". Ransley samples are obtained from a Ransley mold, shown schematically in Fig. 5, originally invented by Ransley and his co-workers to produce samples for measuring the hydrogen content of a melt from the solidified casting using a standard vacuum fusion technique [5]. The mold is specially designed to prepare castings that are porosity-free and which retain the hydrogen con-

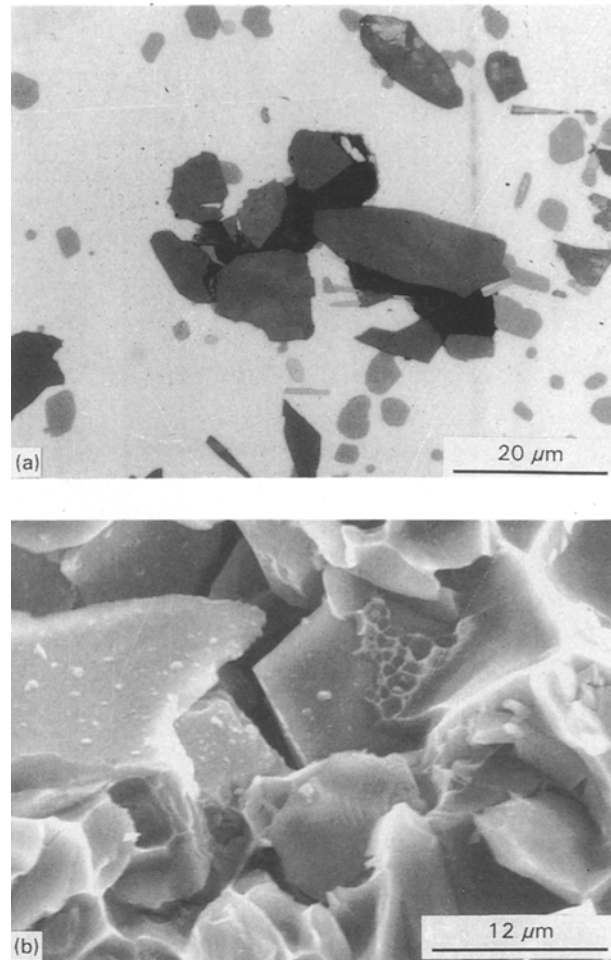


Figure 4 Cavities formed in the composite due to improper feeding: (a) optical microstructure; (b) SEM fracture surface.

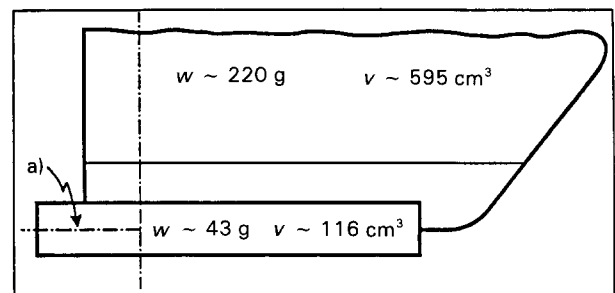


Figure 5 Schematic diagram of Ransley mold [9]; w = weight, v = volume (see text for details).

tent of the melt in the solidified samples [12]. A typical Ransley mold is made of one inch-thick copper plates and weighs ca. 5.52 kg, with a casting obtained from it weighing ca. 260 g. The Ransley sample for hydrogen measurements is machined from the lower, cylindrical part of the casting (rectangular part in the schematic diagram), while the larger, upper (wedge-shaped) part, which acts as the riser, is discarded. Prior to casting, the mold is dried by preheating it at 120 °C, then it is allowed to cool to a temperature above room temperature, to avoid moisture pick-up. Cooling rates of the order of 30 °C s⁻¹ are achieved with the Ransley mold (as estimated from dendrite arm spacing measurements of the cast microstructure). According to Fang

and Granger [13], at such cooling rates the porosity should be about 0.05 vol. %, even for a melt hydrogen level as high as 0.3 ml/100 g Al.

The present authors are of the opinion, therefore, that Ransley samples are best utilized to obtain accurate measurements of the hydrogen content for which purpose they were originally designed. To use them for determining the porosity and oxide contents would be misleading. For a proper comparison of porosity/oxide content with mechanical properties the same test bars obtained from Stahl mold castings and used for tensile testings should also be used for the metallographic measurements.

To this end, a systematic investigation was carried out on the 10 vol % SiC reinforced composite of the present alloy, using both "fresh" (as-received) and "recycled" (gates and runners obtained from the fresh material castings) materials and "continuous" (20 min intervals between pourings) and "discontinuous" (no mechanical stirring for 5 min prior to continuous stirring) stirring modes [14]. Samples for metallographic observation were simultaneously prepared from Ransley and Stahl molds for comparison, with the base alloy (A359) being used as reference (no degassing was applied). The results are depicted in Fig. 6. Two main observations could be made: 1. porosity values as obtained from Stahl mold samples are ca. 4–8 times higher than those obtained from Ransley mold samples taken from the same melt; 2. the presence of the SiC reinforcement enhances the nucleation of porosity. The latter observation has been elaborated upon in detail by the authors elsewhere [15].

Similarly, employing Ransley samples for oxide content measurements would also be inaccurate as the Ransley sample is too small (ca. 43 g) compared to a Stahl mold casting (ca. 1600 g) to correctly represent the actual melt conditions, and an interpretation of the tensile properties obtained from Stahl mold test bars in terms of oxide contents observed from Ransley

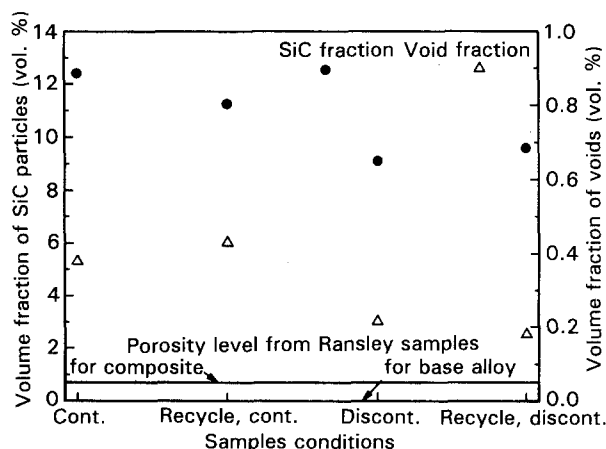


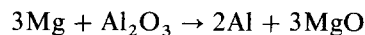
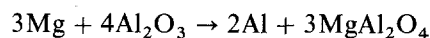
Figure 6 Porosity/void formation in 10 vol % SiC-containing composite measured from samples obtained from Stahl mold and Ransley mold. Results from 359 alloy are superimposed for comparison. C = continuous stirring/fresh material; D = discontinuous stirring/fresh material; CR = continuous stirring/recycled material; DR = discontinuous stirring/recycled material.

samples would not be valid. In addition, the feeding systems in the two molds are also different.

As mentioned above, our investigations on the 10 vol % SiC (p) composite of the present alloy [16] have shown that measurements of the oxide film content from polished sections taken very close to the fracture surface provide a more precise correlation with the tensile properties: the results show that when the oxide volume fraction is ca. 1.4–1.6% the ductility of the 10 vol. % SiC composite reaches its minimum value (less than 0.15%). Direct measurements of the oxide content from the fracture surfaces for correlation with the mechanical properties have been reported by Liu and Samuel [17] and, more recently, by Asselin *et al.* [18].

3.1.3 Melt reactivity

Samuel *et al.* [7] have shown in detail how the presence of high silicon content (ca. 10 wt %) slows down the kinetics of aluminium carbide (Al_4C_3) formation during the melting process in composites of the present alloy. When magnesium (Mg) is present in the alloy matrix, $MgAl_2O_4$ and MgO may also be formed [19] according to the reactions:



the Al_2O_3 being supplied through the oxide film layer that is formed at the melt surface and which can be drawn into the melt at any stage of stirring. In the present composite, energy dispersive X-ray spectrometric (EDX) analysis, Fig. 7a, of a cluster of particles (spinel) similar to that shown in Fig. 4b revealed the presence of magnesium, Fig. 7b, whose concentration, however, was much lower compared to that of aluminium, Fig. 7c.

3.2. Heat treatment

3.2.1. Microstructure

In order to determine the effect of the addition of SiC reinforcement particles to the 359 matrix alloy on the eutectic melting temperature, powdered samples of the

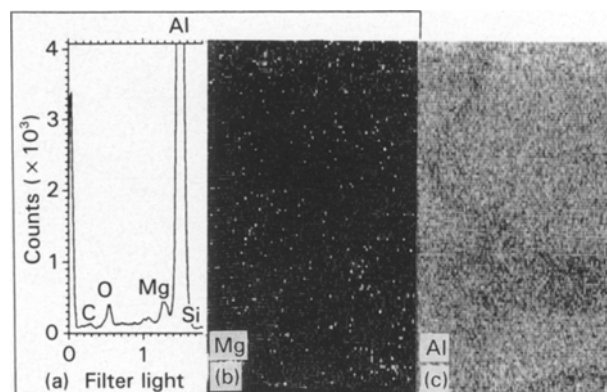


Figure 7 (a) EDX analysis of spinel particles showing distribution of (b) Mg and (c) Al.

composite were subjected to differential scanning calorimetric (DSC) analysis, using a heating rate of ca. $0.1\text{ }^{\circ}\text{C s}^{-1}$. Although all samples displayed a sharp endothermic peak at $576\text{ }^{\circ}\text{C}$ (representing complete melting of the eutectic structure), Fig. 8, the presence of the SiC particles appeared to delay the start of melting, in that the start of melting occurred at ca. $560.3\text{ }^{\circ}\text{C}$ for the base alloy (359), whereas it was raised to $564\text{ }^{\circ}\text{C}$ and further to $568.3\text{ }^{\circ}\text{C}$ for 10 and 20 vol % additions of SiC to the base alloy, respectively. The

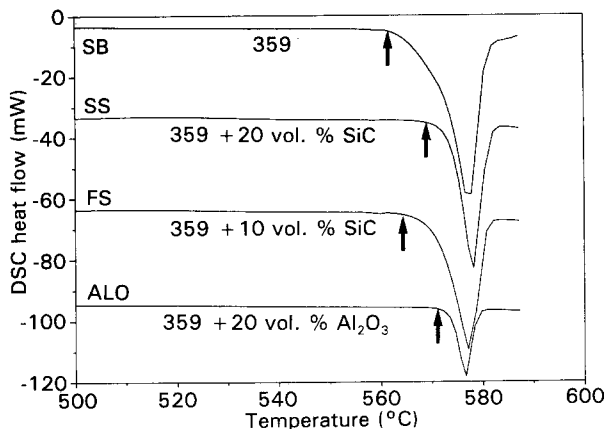


Figure 8 DSC heat flow curves of 359 alloy reinforced by SiC and Al_2O_3 particles; heating rate 0.1 C s^{-1} . Arrows indicate the start of melting of the eutectic silicon in each case.

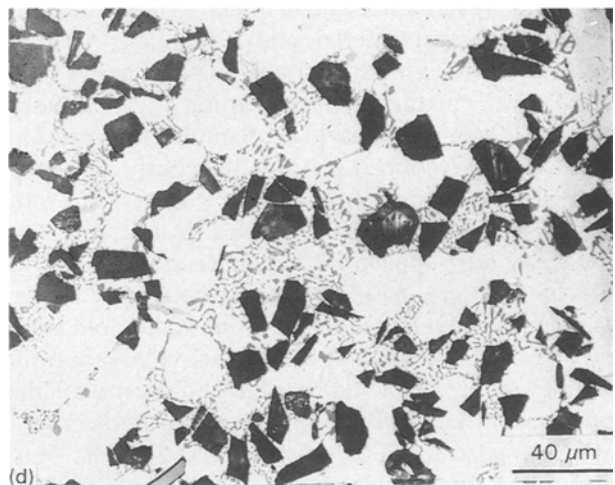
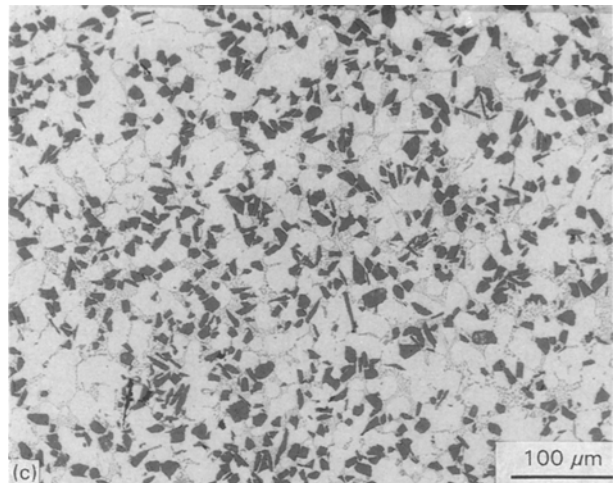
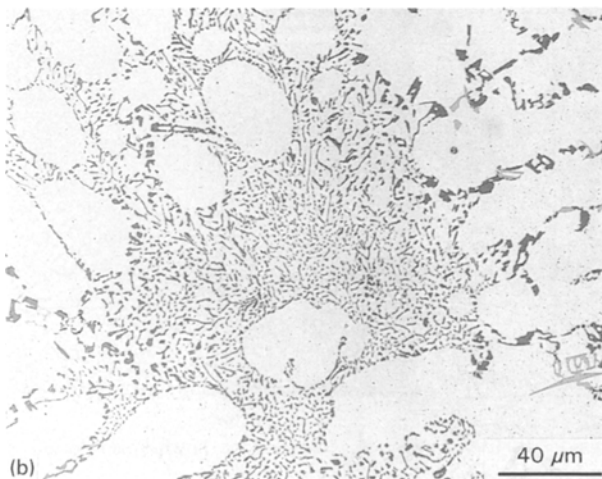
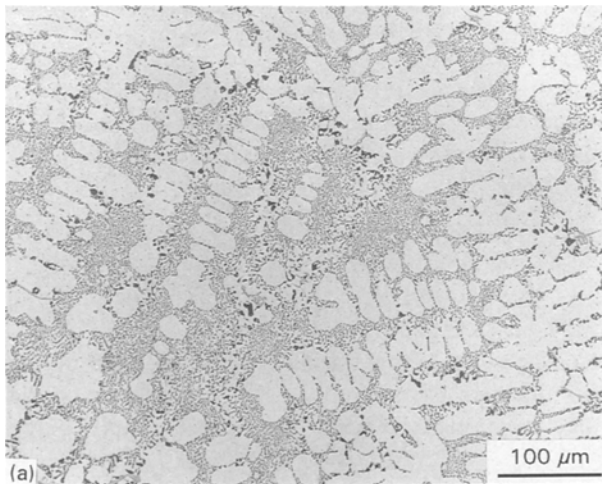


Figure 9 Microstructure of eutectic Si-particles in the as-cast condition for (a) and (b) 359 alloy; (c) and (d) composite.



same effect was also observed in the case of Al_2O_3 reinforcement addition (to be presented elsewhere).

The as-cast microstructures of the base alloy and composite are shown in Fig. 9a and b and 9c and d, respectively. The Sr content in 359 alloy was maintained constant at 150 ppm by adding Al-10 wt % Sr master alloy to the melt from time to time. As mentioned in an earlier publication [20], SiC particles act as sites for preferential nucleation of eutectic Si particles in the as-cast condition. This process of nucleation enhances refinement of the Si particles, as can be observed in Fig. 9.

Table II depicts the eutectic silicon particle characteristics obtained for the base alloy and composite for various heat treatment conditions listed in Table III. Solution treatment at $540\text{ }^{\circ}\text{C}$ for 8 h resulted in complete spheroidization and coarsening of the Si particles, Fig. 10 (cf. to the as-cast condition). Increasing the solution temperature to $550\text{ }^{\circ}\text{C}$ and solution time to 24 h resulted in a further increase in the Si particle mean diameter (or length), Fig. 11. In both cases, the presence of the SiC particles played an important role in controlling the growth rate of the eutectic Si.

It should be noted that the numerical values reported for the composite were affected to some extent by the surface relief of the sample microstructure obtained after polishing, caused by the difference in

TABLE II Characteristics of eutectic Si particles (values in brackets are reduced by 15%)

Alloy type	Condition ^a	Average particle area (μm^2)	Aspect ratio	Particle density (no/mm ²)
359	A	11.04	1.87	5660
	B	8.8	1.44	12326
	C	12.4	1.38	8985
Composite	A	17.6 (15)	1.9	5743
	B	12.3 (10.4)	1.5	9930
	C	18.7 (15.8)	1.4	6261

^a See Table III for corresponding heat treatment details.

TABLE III List of the applied heat treatments

Code	Heat treatment procedure
A	As-cast
B	Samples were solutionized at 540 °C for 8 h and quenched in warm water at 60 °C
C	Samples were solutionized at 550 °C for 24 h and quenched in warm water at 60 °C
D	B + immediate ageing at 155 °C for 5 h
E	B + storage at room temperature for one day prior to ageing at 155 °C for 5 h
F	B + storage at room temperature for two days prior to ageing at 155 °C for 5 h
G	As E, except that the test bars were quenched in cold water at 25 °C at the end of B
H	As E, except that the test bars were stored at - 5 °C for one day prior to ageing at 155 °C for 5 h
I	As E, except that the test bars were aged at 210 °C for 100 h

strength between the SiC particles and the surrounding matrix. Although the image analysis program was modified to remove this relief-related effect it could not be totally avoided. Based on several measurements, it was estimated that this resulted in an increase of ca. 15% in the measured values of the average silicon particle length and area. Thus, in Table II, both obtained and corrected values are given for the composite samples, where the values in parentheses are the obtained values reduced by 15%.

Comparing Tables I and II shows that a 90 ppm level of Sr was sufficient to obtain the same degree of refinement (of the eutectic silicon) in the composite alloy as that achieved in the base 359 alloy with a 150 ppm Sr content.

In Table II, it can also be observed that the number of silicon particles is less in the composite sample than in the base alloy in the solution treated conditions. While the numbers themselves should not be considered as absolute, since only a certain number of fields of observation are chosen to scan the entire specimen surface in a regular, periodic fashion, the trend, nevertheless, is apparent. This can be understood by referring back to the as-cast microstructures of Fig. 9. The base alloy specimen, Fig. 9a and b, clearly shows the presence of large interdendritic re-

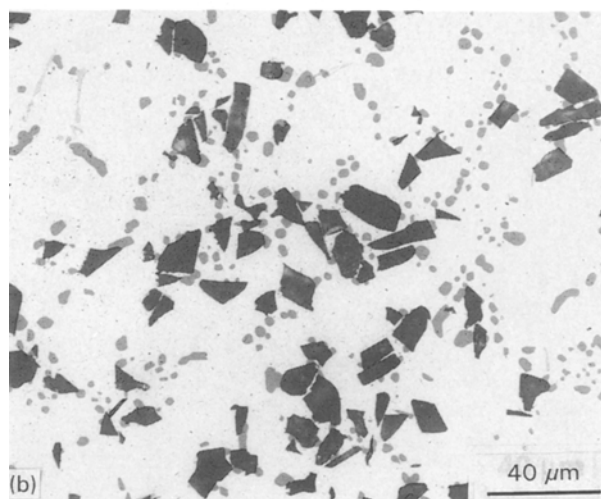
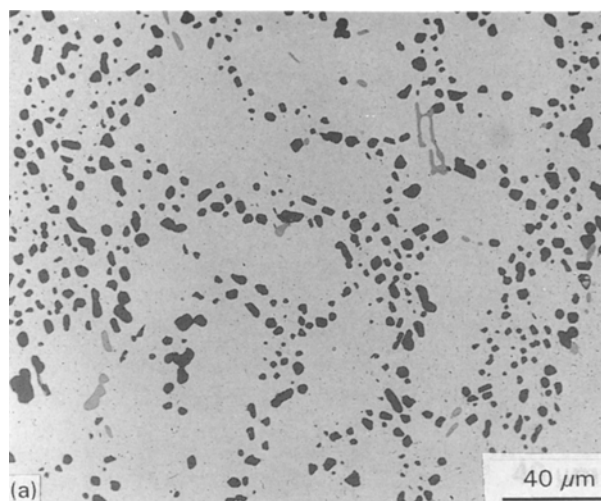


Figure 10 Microstructure of eutectic Si particles solutionized at 540 °C for 8 h for (a) 359 alloy and (b) composite.

gions where a concentration of the silicon particles occurred. These regions are randomly dispersed over the specimen surface. The composite sample, Fig. 9c and d, on the other hand, displays a much more uniform distribution of the interdendritic regions, the regions themselves being much smaller than those seen in Fig. 9a. Also, in the composite, these interdendritic regions have to accommodate both Si particles and the SiC reinforcement. Thus, effectively, on a one-to-one basis, there will be fewer Si particles observed in the composite sample than in the base alloy for the same area (or number of fields) scanned. However, because the silicon level remains the same in both alloys, the silicon particle distribution will have to be rearranged to accommodate the same silicon level in the composite. This appears to be accomplished by the uniform/smaller interdendritic region pattern exhibited by the solidification structure of the composite, and would also explain the shift in the start of melting points for the composite samples shown in Fig. 8. Thus, in addition to the refining effect on the Si particles, the presence of the SiC particles is also beneficial in this respect.

The work of Shivkumar *et al.* [2] demonstrates that the optimum solution time for modified 356 alloy at

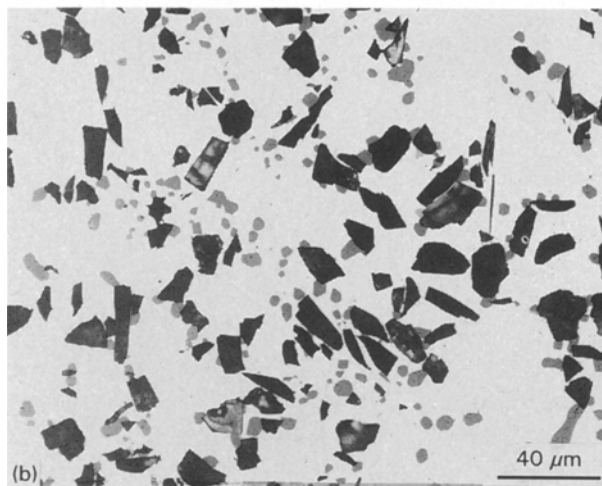
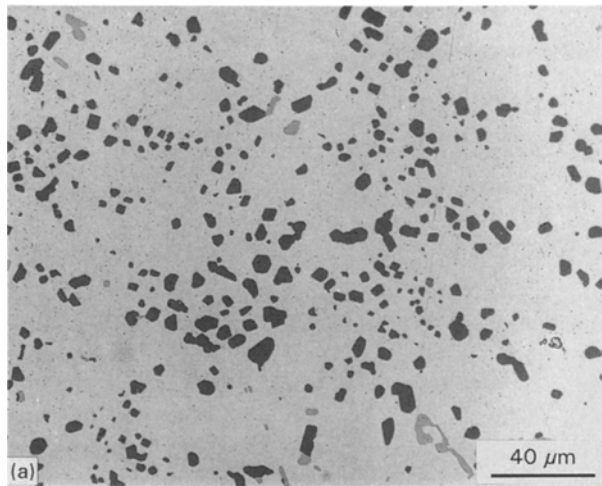


Figure 11 Microstructure of eutectic Si-particles solutionized at 550 °C for 24 h for (a) 359 alloy and (b) composite.

540 °C is of the order of 50–100 min in permanent mold castings (Stahl mold) and is shortened to 25–50 min at 550 °C. When the solution temperature is increased above 540 °C it becomes imperative that the temperature (in castings being heat treated) be controlled precisely in order to avoid grain boundary melting.

3.2.2. Tensile properties

It has been reported that the addition of SiC particles to aluminium alloys improves their yield strength and Young's modulus. However, it also results in a significant reduction in their ductility and fracture toughness. Flom and Arsenault [21] have related such reduction in ductility to an inhomogeneous distribution of the SiC particles and void initiation at the reinforcement–matrix interface during straining to a weak interfacial bond.

The solution treatment homogenizes the as-cast microstructure and minimizes segregation of alloying elements in the casting [22]. Following solutionizing, the casting is usually quenched in water. The purpose of quenching is to suppress the formation of the equilibrium Mg_2Si phase during cooling and retain the maximum amount in solution to form a super-saturated solid solution at room temperature.

Taya *et al.* [23] have performed a parametric study on the strengthening of a 6061/SiCp particulate metal-matrix composite by quenching. They attributed the strengthening to two mechanisms: strengthening due to coefficient of thermal expansion mismatch (between the metal matrix and reinforcement particles) strain induced by quenching, and that due to back stress, which is the average internal stress in the matrix as a result of the particulates resisting the plastic flow of the matrix.

A rapid quenching will ensure that all Mg_2Si is retained in solid solution, and the highest strength attainable is obtained with fast quench rates. The quench rate, however, cannot be increased indefinitely since distortion and residual stresses are introduced into the casting at high cooling rates [24].

Tsukuda *et al.* [25] have studied the effects of pre-ageing at 25 °C on the tensile properties in T6-tempered test bars obtained from permanent mold castings of Al-7% Si alloys. They concluded that storing the samples results in a reduction in both YS and UTS. This decrease is accompanied by a corresponding enhancement of ductility and impact toughness. Furthermore, Ghate *et al.* [26] have found that the effect of pre-ageing is more pronounced at higher Mg contents.

During artificial ageing of Al–Si–Mg alloys the precipitated phase is Mg_2Si . A four-stage process is suggested as follows [27]:

1. precipitation of G-P zones;
2. intermediate phase β' - Mg_2Si , together with a homogeneous precipitation;
3. intermediate phase β' - Mg_2Si together with a heterogeneous precipitation;
4. equilibrium phase β - Mg_2Si structure.

Fig. 12a to e summarize the tensile properties obtained from both the base alloy and composite after various heat treatments (see Table III). Complete details of the tensile properties as a function of ageing temperature and time are to be published elsewhere [28]. The main points inferred from these results are given below.

3.2.2.1. Addition of SiC particulates. The presence of the SiC reinforcement increases the Young's modulus from 10.5 Msi (359 base alloy) to 14.4 Msi (ca. 40% increase, independent of the applied heat treatment). Although the particles do not exert any significant influence on the UTS value of the 359 alloy, the YS is increased by ca. 30–40% in the as-cast condition as well as after heat treatment. The ductility and quality index [$Q(\text{ksi}) = \text{UTS}(\text{ksi}) + 21.9 (\text{Log EL})$] of the 359 alloy, however, are drastically reduced by ca. 80 and 50%, respectively, with the addition of the SiC particles.

3.2.2.2. Solution treatment. As mentioned in Table III, two solution treatments were applied, namely, B and C. Prolonged solutionizing at 550 °C (compared to 8 h at 540 °C) resulted in an increase in both YS and

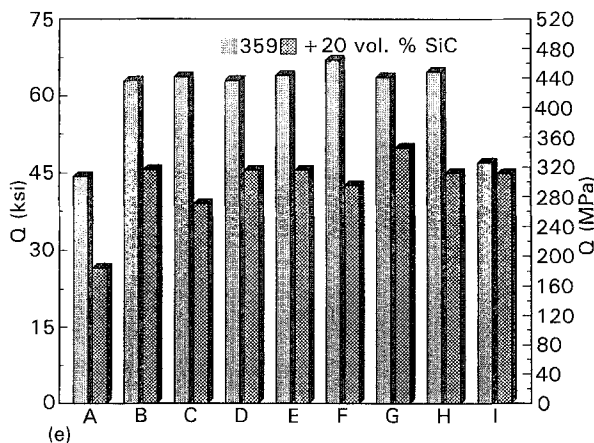
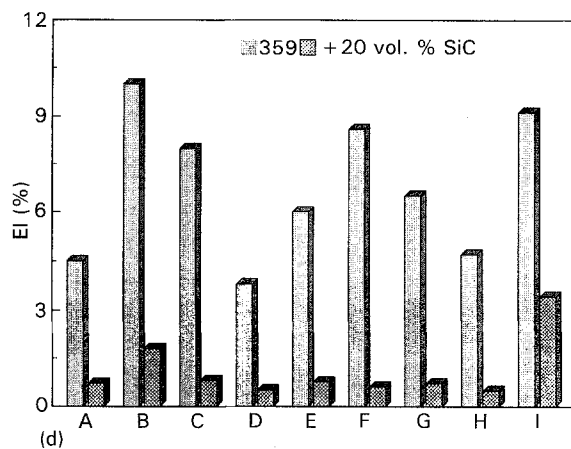
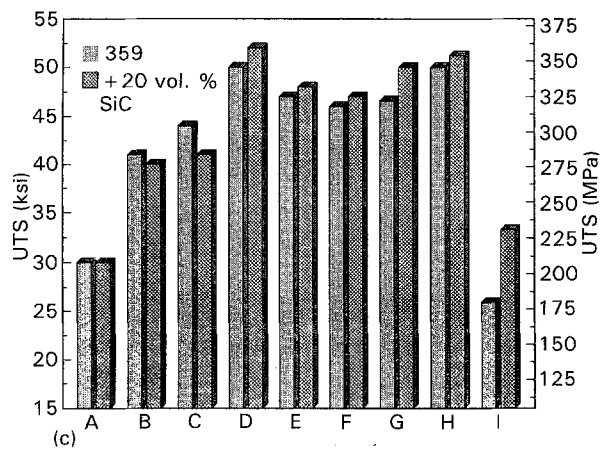
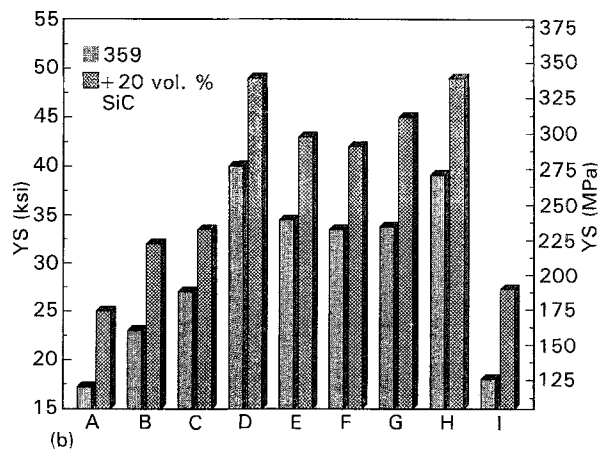
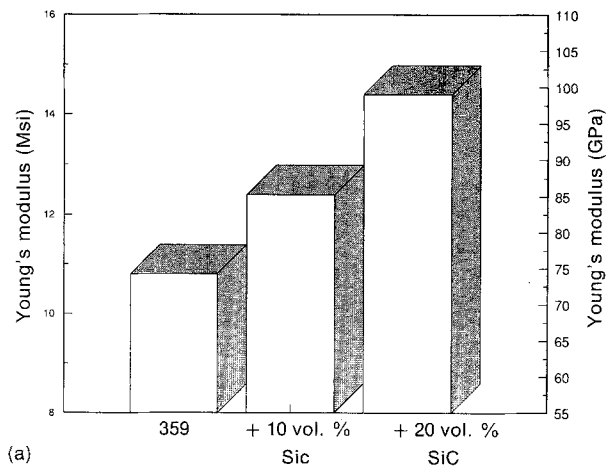


Figure 12 Effect of the addition of 20 vol. % SiC particles on (a) Young's modulus, (b) YS, (c) UTS, (d) EL and (e) Q values. Each value is the average obtained from 8–10 test bars.

UTS values by ca. 10% (359) and ca. 4% (composite), while the ductility was reduced by 20 and 50%, respectively. Therefore, treatment C was not recommended. In addition, at the higher temperature, there is always the need for precise monitoring of the temperature in order to avoid grain boundary melting. In any case, solution treatment B significantly improved the strength, ductility and the quality index of the as-cast product, and was therefore adopted for subsequent heat treatment procedures.

3.2.2.3. *Quenching medium.* Two quenching media were used, i.e. cold (25 °C) and warm (60 °C) water. The quenching time was less than 10 s in both cases. The tensile properties, however, were not much affected

(less than 5%). Increasing the quench time more than that (through the use of boiled water or still air as the quenching medium) had a harmful effect on the mechanical properties.

3.2.2.4. *Artificial ageing.* Maximum increase in YS (100–135%) and UTS (70–80%) was achieved when the as-cast material was solution treated and immediately aged at 155 °C for 5 h with no pre-ageing. This process resulted in a slight decrease in the alloy ductility. However, the quality index (Q) being the sum of UTS and ductility, high values of Q were attained in the T6 temper.

3.2.2.5. *Pre-ageing/storing.* Storing the quenched test bars in still air for one day (treatment E) resulted in a noticeable decrease in the alloy strength with a pronounced effect on the YS (ca. 14% versus 6% for UTS). As expected, this process was associated with ca. 40% increase in the alloy/composite ductility. These values are in good agreement with those reported by Chamberlain and Zabek [29]. Neither storing for a longer time (i.e. two days, treatment F) nor quenching in cold water (treatment G) produced further changes in the alloy/composite tensile properties.

Storing at temperatures below 0°C (i.e. - 5°C, treatment H) diminished the effect of pre-ageing.

Maximum attainable ductility of the composite (3.5%) was achieved on ageing at 210°C for 100 h (test bars were stored for one day at 25°C, treatment I). As expected, the YS and UTS values were almost half of those obtained from treatment D (5 h at 155°C, with no pre-ageing). The latter represents the customary heat treatment applied to this category of alloys.

4. Conclusions

From this study of the influence of various melting, casting and heat treatment parameters on the tensile properties of an Al-10 wt % Si-0.6 wt % Mg/SiC/20p composite and its base alloy (359), the following may be concluded.

1. The shrinkage obtained in permanent (Stahl) mold castings of composites containing a high volume fraction of SiC reinforcement particles (20 vol %) can be reduced or eliminated through the use of a proper mold temperature and appropriate mold coating materials that enhance the feedability of the molten composite.

2. Melt-temperature, hydrogen level, cleanliness and stirring variously affect the quality of the obtained composite casting and hence its properties.

3. Proper choice of metallographic sample for measurement of porosity/oxide-inclusion content is important to obtain any realistic correlation with the tensile properties. Samples obtained from test bar gauge lengths of fractured test bar castings are thus more precise than Ransley samples obtained from a Ransley mold casting of the same melt (cf. porosity volume fractions of 0.4–0.6% with ca. 0.05% obtained in the two cases).

4. The presence of the SiC reinforcement particles is beneficial in two respects: (a) the particles act as preferential sites for the nucleation of the eutectic silicon particles, leading to an overall refinement of the latter and lowering the amount of strontium modifier required from 150 to 90 ppm to achieve the same level of refinement in the composite as in the base alloy; (b) a more uniform redistribution of the silicon particles is obtained (cf. the large, irregular interdendritic regions of eutectic silicon in the base alloy).

5. The addition of 20 vol % SiC particles to the base alloy affects the Young's modulus and yield strength by an increase of ca. 30–40%, marginally affects the ultimate tensile strength, but considerably reduces the ductility by almost 80%. Both base alloy and composite, however, show a similar response to the different heat treatments applied.

Acknowledgements

The authors would like to thank Duralcan Canada, Usine Dubuc, Chicoutimi, Québec for supplying the composite material. They also wish to thank Mr C. Cooney of KRDC, Alcan International Ltd, Kingston, Ontario for carrying out the DSC analysis. The financial support received from the Natural Sciences and Engineering Research Council of Canada, the Fond-

ation de l'Université du Québec à Chicoutimi and the Société d'électrolyse et de chimie Alcan (SECAL) is gratefully acknowledged.

References

1. D. APELIEN, S. SHIVKUMAR and G. SIGWORTH, *AFS Trans.* **97** (1989) 727.
2. S. SHIVKUMAR, S. RICCI, B. STEENHOFF, D. APELIEN and G. SIGWORTH, *AFS Trans.* **97** (1989) 791.
3. D. E. HAMMOND, *AFS Trans.* **97** (1989) 887.
4. F. H. SAMUEL, A. M. SAMUEL and H. LIU, *AFS Trans.* (in press).
5. C. DUPUIS, Z. WANG, J.-P. MARTIN and C. ALLARD, *Light Met.* (1992) 1055–68.
6. ASTM Standards, "Standard specification for aluminum alloy permanent mold castings", 02.02 (1990) 104.
7. A. M. SAMUEL, H. LIU and F. H. SAMUEL, *Compos. Sci. Technol.* **49** (1993) 1.
8. J. BOUTIN and C. E. GALLERNAUT, Report no. AR-89/0028, Arvida R&D Centre, Alcan International Limited, Jonquièrre, Québec, Canada, July 1989.
9. R. PROVENCHER, G. RIVERIN and C. CELIK, "Advances in production and fabrication of light metals and metal matrix composites", edited by M. Avedesian, L. J. Larouche and J. Masounave (The Canadian Institute of Mining, Metallurgy and Petroleum, Montreal, 1992) p. 589.
10. D. L. ROSE, B. M. COX and M. D. SKIBO, *AFS Trans.* (in press).
11. A. D. McLEOD, in Proceedings of the ASM International Conference on Fabrication of Particulates Reinforced Metal Composites, Montreal, September 16–19, 1990, p. 25.
12. C. E. RANSLEY and D. E. J. TALBOT, *J. Inst. Met.* **84** (1955–56) 445.
13. Q. T. FANG and D. A. GRANGER, *AFS Trans.* **97** (1989) 989.
14. H. LIU and F. H. SAMUEL, *AFS Trans.* (in press).
15. A. M. SAMUEL and F. H. SAMUEL, *Metall. Trans. A* **24A** (1993) 1857.
16. F. H. SAMUEL, H. LIU and A. M. SAMUEL, *Metall. Trans. A* **24A** (1993) 1631.
17. H. LIU and F. H. SAMUEL, Internal report, Arvida R&D Centre, Alcan International Limited, October 1991.
18. D. ASSELIN, M. BOUCHARD and R. PROVENCHER, "Development and applications of ceramic and new metal alloys", edited by R. A. L. Drew and M. Mostaghaci (The Canadian Institute of Mining, Metallurgy and Petroleum, Montreal, 1993) p. 233.
19. N. WANG, Z. WANG and G. C. WEATHERLY, *Metall. Trans. A* **23A** (1992) 1423.
20. F. H. SAMUEL and A. M. SAMUEL, *Metall. Trans. A* (in press).
21. Y. FLOM and R. J. ARSENAULT, *Acta Metall.* **37** (1989) 2413.
22. F. PARAY and J. E. GRUZLESKI, *Cast Metals* **5** (1993) 187.
23. M. TAYA, K. E. LULAY and D. J. LLOYD, *Acta Metall. Mater.* **39** (1991) 73.
24. R. W. BRUNER, in the Proceedings of the Conference "Heat treatment of Al-alloy castings: The state of the art", Detroit, MI, 1979, 209.
25. M. TSUKUDA, S. KOIKE and K. ASANO, *J. Jpn. Inst. Light Metals* **28** (1978) 531.
26. G. S. GHATE, K. S. RAMAN and K. S. S. MURTHY, in Proceedings of the Conference "International conference on aluminum-85 (INCAL)", New Delhi, India, 1985, 485.
27. J.-P. COTTU, J.-J. COUDERE, B. VIGUIER and L. BERNARD, *J. Mater. Sci.* **27** (1992) 3068.
28. F. H. SAMUEL and A. M. SAMUEL, Unpublished work.
29. B. CHAMBERLAIN and V. J. ZABEK, *AFS Trans.* **81** (1973) 322.

Received 21 December 1993
and accepted 10 January 1994